



Viscosity behaviour of water-emulsified engine oil for hydrogen internal combustion engine applications

Jon Pow Wan ¹, Nur Aisya Affrina Mohamed Ariffin ^{1*}, William W. F. Chong ^{1,2}, Jo-Han Ng ³

¹ Faculty of Mechanical Engineering, Universiti Teknologi Malaysia, 81310 UTM Skudai, Johor, MALAYSIA.

² Institute for Sustainable Transport (IST), Universiti Teknologi Malaysia, 81310 UTM Skudai, Johor, MALAYSIA.

³ Carbon Neutrality Research Group, University of Southampton Malaysia, MALAYSIA.

*Corresponding author: nuraisyaafrina@graduate.utm.my

KEYWORDS

Water-in-oil emulsions
Viscosity-temperature
behaviour
Vogel-Fulcher-Tammann
(VFT) model
Boundary lubrication
Hydrogen-fuelled internal
combustion engines
(H₂ICEs)

ABSTRACT

Hydrogen-fuelled internal combustion engines (H₂ICEs) emit significant quantities of water vapour, which can condense and accumulate in the crankcase. Under mechanical agitation, this moisture may form water-in-oil emulsions, potentially impairing lubricant performance. This study simulates such conditions by emulsifying synthetic SAE 5W-40 engine oil with up to 40 wt% deionised water, to mimic shear-induced water contamination in H₂ICEs. For the emulsified lubricants, viscosity increased with water content, and the Vogel-Fulcher-Tammann (VFT) equation effectively described their temperature dependence. Reduced viscosity-temperature sensitivity observed at higher water levels resembled high-viscosity-index behaviour, indicating enhanced thermal stability. Tribological tests revealed that moderate water content (less than 20 wt%) decreased friction and wear due to increased film thickness, attributing to higher viscosity. However, corrosion escalated sharply beyond 20 wt% water contamination, posing long-term durability risks. These findings establish critical thresholds, where water contamination shifts from beneficial to detrimental. The results emphasised the necessity to optimise lubricant formulations for H₂ICEs by balancing viscosity, wear protection, and corrosion resistance in moisture-rich environments.

Received 20 June 2025; received in revised form 26 September 2025; accepted 29 October 2025.

To cite this article: Wan et al. (2025). Viscosity behaviour of water-emulsified engine oil for hydrogen internal combustion engine applications. *Jurnal Tribologi* 47, pp.73-86.

1.0 INTRODUCTION

In the global pursuit of reducing carbon emissions, hydrogen-powered internal combustion engines (H₂ICEs) have emerged as a promising transitional solution. Unlike conventional fossil fuels, hydrogen combustion yields no tailpipe carbon dioxide (CO₂) emissions, positioning it as a cleaner solution (Onorati et al., 2022). H₂ICEs offer the advantage of leveraging existing engine technologies and infrastructure, making them a cost-effective and rapidly deployable option, particularly for heavy-duty vehicles, where battery-powered electric solutions face range and weight limitations (Onorati et al., 2022; Rahmani et al., 2023). However, using hydrogen as a fuel introduces specific tribological and lubrication challenges not typically encountered in gasoline and diesel engines.

One of the primary concerns is the significant amount of water vapour produced during hydrogen combustion (Chen et al., 2021; Rahmani et al., 2023). Under H₂ICEs' operating conditions, this vapour readily condenses and infiltrates the crank case, where mechanical shear and thermal cycling promote the formation of water-in-oil emulsions. Reports indicate that such contamination can reach levels of up to 24 wt%, particularly under high-humidity environments or prolonged idling conditions (Butcher et al., 2023). These emulsions can significantly alter the lubricant's physicochemical properties by affecting the viscosity, thermal stability, film formation and corrosion resistance (Zhou et al., 2024). Additionally, a study by Stępień (2021) reported that the use of hydrogen presents other performance challenges, including early pre-ignition, knocking combustion, and backfire.

Unlike fuel dilution, which typically decreases viscosity, water contamination can induce complex, non-linear changes in oil rheology due to hydrogen bonding, microstructural rearrangements, and phase separation at elevated concentrations. While some studies suggest that small amounts of emulsified water may temporarily stabilise viscosity or enhance cooling, excessive moisture generally compromises lubrication performance (Bhosale et al., 2014). Hydrogen combustion has been shown to accelerate engine degradation (Amat Ventayol et al., 2025; Wang et al., 2023). Synthetic oil emerged as the prevalent choice for H₂ICEs among lubricants due to its enhanced thermal stability and shear resistance over a wide temperature range (Sazzad et al., 2024). Yet even minimal moisture in this oil can trigger harmful consequences, undermining its effectiveness in lubricating engine parts and safeguarding against wear and corrosion. Lubricating oils, essential for reducing friction and preventing wear in rotating equipment, undergo property changes during operation that can compromise the equipment's lifespan (Sharma et al., 2020).

Lubricants typically comprise 70-90% base oil and 10-30% functional additives, such as viscosity modifiers, antioxidants, and anti-wear agents (Ayeni et al., 2021). These additives are vulnerable to degradation in water, particularly under the harsh conditions typical of engine operation—high temperature, pressure, and continuous shear. Consequently, understanding the impact of water contamination on oil properties is essential for maintaining engine reliability and prolonging lubricant life (Domínguez-García et al., 2022).

To address this knowledge gap, the present study serves as a first-phase investigation focused on evaluating the bulk performance of engine oils under simulated crankcase water contamination. Emulsions were prepared by blending distilled water at concentrations ranging from 5 to 40 wt% into a commercially available fully synthetic SAE 5W-40 engine oil. This oil grade was chosen for its widespread use and availability rather than as a specific recommendation for H₂ICEs. Viscosity changes were characterised across a broad temperature range using the Vogel-Fulcher-Tammann (VFT) empirical model, and tribological and corrosion

tests (including copper strip analysis) were conducted to evaluate mechanical protection and chemical stability. The findings provide practical insights into the rheological and degradation behaviour of lubricants under water exposure or ingress and help define critical water tolerance thresholds relevant to H₂ICE operation.

1.0 MATERIAL AND EMULSION PREPARATION

A commercially available fully synthetic engine oil from Shell (Malaysia) was tested in this study, which is SAE 5W-40. Emulsions were prepared by blending the oil with deionised water at varying concentrations from 5 to 40 wt%. The selected water concentrations were chosen to represent realistic and accelerated crankcase contamination scenarios in H₂ICEs based on literature findings (Butcher et al., 2023).

The neat engine oil, free from water contamination, served as the base reference. The emulsification process involved two main stages. First, the oils and the designated amount of deionised water were mixed using a magnetic stirrer at 400 rpm for 10 minutes. It was ensured that a vortex formed during stirring to promote homogeneous dispersion of water droplets within the oil matrix. Then, the mixture underwent an ultrasonication process at 60 °C for two hours, forming a stable water-in-oil emulsion. This step facilitated the formation of a stable water-in-oil emulsion by reducing the size of the dispersed water droplets and enhancing their uniform distribution throughout the continuous oil phase. All prepared samples, including the neat engine oil, were stored in sealed test tubes at ambient room temperature.

2.0 VISCOSITY MEASUREMENT AND VOGEL'S EQUATION

The dynamic viscosity of the samples was measured using a digital rotary viscometer (Model NDJ-8S) with the selection of rotor #0 for the proper viscosity range. To ensure accurate and reliable measurements, the rotational speed of the rotor was adjusted such that the instrument's torque reading consistently remained within the optimal range. The viscosity measurement started at room temperature (25 °C) for all samples and increased to 80 °C. Care was taken during each measurement to ensure the sample volume was sufficient to submerge the rotor and fill the viscometer tube. This was particularly crucial at elevated temperatures, where the potential for evaporation could otherwise compromise measurement consistency and accuracy. All measurements were performed under steady-state conditions, with precise temperature control to minimise fluctuations.

Vogel-Fulcher-Tammann (VFT) equation was used to correlate the measured viscosity with temperature. This is an empirical formula used to describe the temperature dependence of viscosity in supercooled liquids, polymers, and other complex fluids like emulsified lubricants (Garca-Coln et al., 1989). The relationship can be described using Equation (1):

$$\eta(T) = \eta_0 e^{\left(\frac{B}{T-T_0}\right)} \quad (1)$$

Where $\eta(T)$ is the dynamic viscosity at absolute temperature T (in Kelvin), η_0 is the viscosity at infinite temperature, B is the flow activation constant and T_0 is the Vogel temperature. Based on Equation (1), η_0 , B and T_0 are three adjustable parameters to analyse the viscosity dependency on temperature change. In this study, these parameters were determined through non-linear

curve fitting of the experimental viscosity data, achieving a fitting error of less than 5%, thereby validating the applicability of the VFT model to the emulsified engine oil systems investigated.

3.0 COPPER STRIP CORROSION TEST

The corrosiveness of each sample was tested using the Copper Strip Corrosion Test, following modified ASTM D130 as described in Shi and Larsson (2016). The copper strips (15 ± 1 mm long, 13 ± 1 mm wide and 3 ± 1 mm thick) were manually polished using 120-grit (medium) followed by 220-grit (fine) silicon carbide abrasive paper for consistent finishing. The polished strip was cleaned with acetone to remove any debris and contamination on the surface. The strips were immediately immersed, ensuring that at least 5 mm of the strip was fully submerged in a test tube containing the samples. The test tubes were placed in a controlled oil bath maintained at 100 ± 1 °C for three hours. After heating, the strips were removed and cleaned with acetone to eliminate any remaining lubricant. The corrosiveness was visually inspected by comparing the appearance against the ASTM Copper Strip Corrosion Standard. Each test was repeated three times to ensure repeatability, and the most representative results were reported.

4.0 FRICTION TESTING

The friction test was conducted using a custom-made ball-on-disk tribometer, as shown in Figure 1. Each friction test incorporated an AISI 52100 steel ball (\varnothing 6 mm) with an AISI 304 stainless steel disk (\varnothing 50 mm, thickness ± 1 mm). The arithmetic average surface roughness (R_a) for the ball and disk was $0.15 \mu\text{m}$ and $0.3 \mu\text{m}$, respectively.

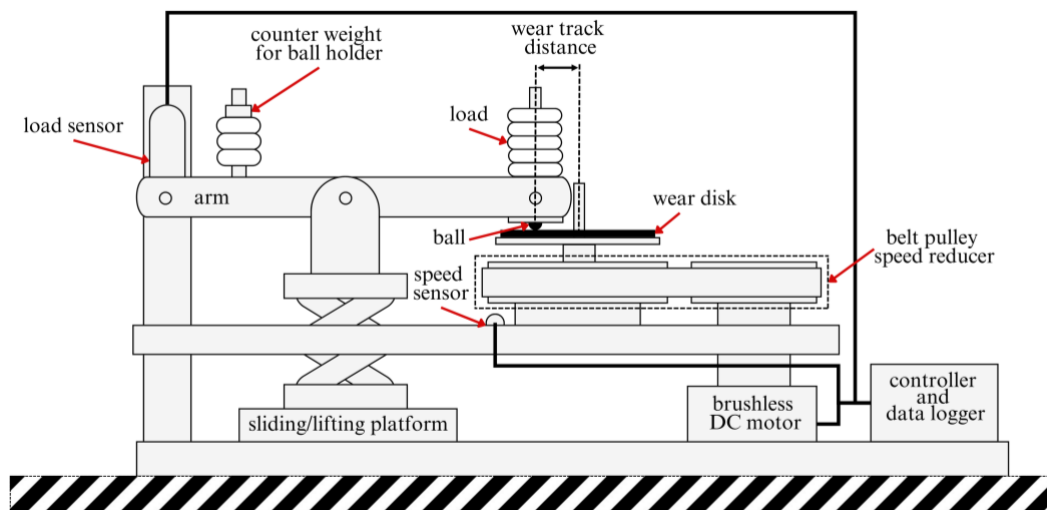


Figure 1: Custom-made ball-on-disk tribometer.

Before each friction test, the ball and disk underwent a pre-treatment process following Lee et al. (2022) and Mohamed Ariffin and Chong (2024) to improve surface wettability. The procedure involved rinsing with distilled water, ultrasonicing in acetone and immersing in ethanol. The

disk was oven-dried at 30 °C for 30 minutes before the actual friction test to evaporate the ethanol. Then, the disk was cooled naturally at room temperature before being spin-coated with 0.5 mL of the sample at 3500 rpm for 30 s. The actual friction test was conducted following the test conditions in Table 1.

For each applied load, the test duration was fixed at 255 s. A run-in stage was first conducted at 60 g load and 1000 rpm for 60 s to stabilize the contact and remove initial surface irregularities, ensuring that 255 s was sufficient to obtain steady and reproducible tribological behaviour (Mohamed Ariffin et al., 2024). Each test was repeated three times for consistency purposes. At the end of the friction test, the steel ball wear scar diameter was measured using an optical microscope to assess wear performance.

Table 1: Experimental conditions for friction testing SAE 5W-40 oil with varying water concentrations.

Parameter	Value
Speed (rpm)	500
Load (g)	80 – 200 (increment of 20 g)
Duration per load (s)	255

5.0 RESULTS AND DISCUSSION

Figure 2 presents the variation of dynamic viscosity with temperature for SAE 5W-40 engine oil blended with different concentrations of deionised water. All samples exhibit a general decrease in viscosity with increasing temperature, which is attributed to the thermal weakening of intermolecular forces within the lubricant matrix (Hemmat Esfe et al., 2022; Vasisht et al., 2014). Notably, dynamic viscosity increases proportionally with water concentration at all temperatures. For example, at 298 K (ambient temperature), the sample containing 40 wt% water records the highest viscosity of 252.6 mPa·s. This increase is likely due to enhanced hydrogen bonding and microstructural changes introduced by water incorporation (Musa Abubakar et al., 2018). Theoretical viscosities, obtained by fitting the VFT equation (in Equation 1), are shown as trendlines for each curve. The close agreement between experimental and fitted data confirms the VFT model's suitability for describing the temperature-dependent behaviour of these water-contaminated lubricants.

In summary, the addition of deionised water to SAE 5W-40 oil results in increased viscosity. This behaviour indicates higher load-bearing capacity across a broad temperature range. Curve-fitting using the VFT equation (given in Equation 1) produced optimised values for the three Vogel parameters, as summarised in Table 2. These values were selected based on a root mean squared error (RMSE) of less than 5% relative to the experimental viscosity data, ensuring the accuracy and reliability of the model. Figure 3 presents the optimised VFT parameters as a function of deionised water concentration, visually representing the relationship between water content and viscosity behaviour.

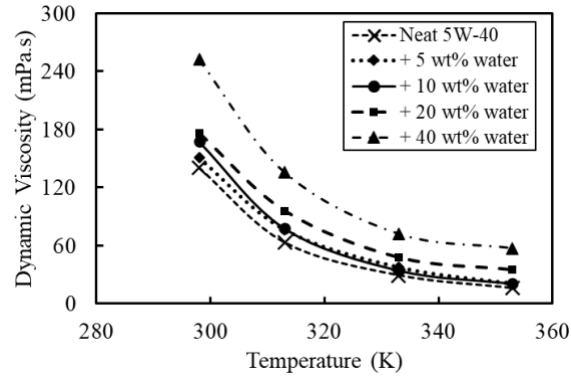


Figure 2: Viscosity as a function of temperature for SAE 5W-40 oil blended with varying concentrations of deionised water.

Table 2: VFT model parameters — dynamic viscosity at infinite temperature (η_0), flow activation constant (B), and Vogel temperature (T_0) — for SAE 5W-40 oil blended with varying concentrations of deionised water.

Sample	η_0 (mPa·s)	B (-)	T_0 (K)
Neat 5W-40	0.4	582.5	200.5
+ 5 wt% water	0.1	1026.0	154.5
+ 10 wt% water	0.3	657.4	191.0
+ 20 wt% water	1.9	429.6	203.6
+ 40 wt% water	9.2	208.2	235.2

As shown in Figure 3(a), the dynamic viscosity at infinite temperature (η_0) increases markedly with water concentration, especially at higher water contents (20 wt% and 40 wt%). The highest η_0 of 9.2 mPa·s, observed for SAE 5W-40 emulsified with 40 wt% water, indicates that higher water additions promote extensive hydrogen bonding (Musa Abubakar et al., 2018), increasing viscous resistance. The flow activation constant (B), shown in Figure 3(b), reflects the sensitivity of viscosity to temperature. Initially, the introduction of 5 wt% water raises B by 76.1% (from 582.5 to 1026.0), suggesting that even a small amount of water significantly enhances the temperature dependence of the lubricant. This behaviour may result from an unstable microstructure highly susceptible to thermal disruption (Cafolla & Voitchovsky, 2020; Røn & Lee, 2014). With further increases in water concentration, B decreases steadily, reaching a minimum of 208.2 at 40 wt% water. This decline implies that higher water content stabilises the emulsion structure by forming a more robust hydrogen-bonded network that is less prone to thermal breakdown.

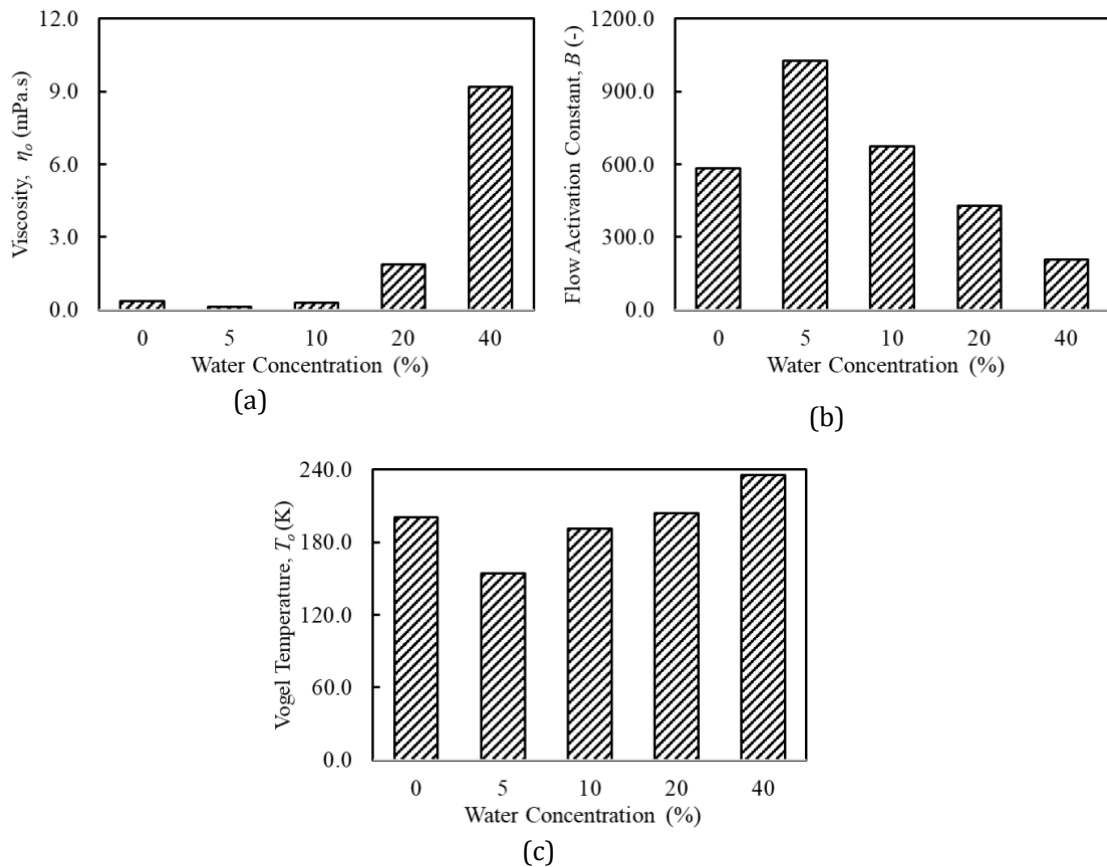


Figure 3: Variation of VFT parameters with water concentration in SAE 5W-40 oil: (a) dynamic viscosity at infinite temperature (η_0), (b) flow activation constant (B), and (c) Vogel temperature (T_0).

Figure 3(c) illustrates that the Vogel temperature (T_0) rises gradually with water concentration, from 200.5 K for the neat oil to 235.2 K at 40 wt% water. The overall increase in T_0 indicates enhanced cohesive energy within the system, supporting the hypothesis that stronger intermolecular interactions, such as hydrogen bonding, develop at higher water levels. The slight decrease at 5 wt% water may reflect a partial disruption of the original oil structure. This is counterbalanced by forming more stable, water-oil hydrogen-bonded networks at greater water contents.

Figure 4 illustrates the corrosiveness of SAE 5W-40 oil and its emulsions containing varying water concentrations, based on the post-test appearance of copper strips. Corrosiveness increased markedly with water content, which can be attributed to the greater availability of oxygen and polar water molecules that facilitate oxidative reactions and surface corrosion (Noori et al., 2018). At a small water concentration (less than 20 wt%), the corrosiveness is at 1a (slightly tarnished as per ASTM D4048). Beyond 20 wt%, the copper strips exhibited pronounced discolouration, signifying a substantial increase in corrosive activity. This trend reflects the diminished chemical stability of the emulsion at higher water contents, which may promote the

formation of corrosive by-products and accelerate the degradation of metallic engine components over time.

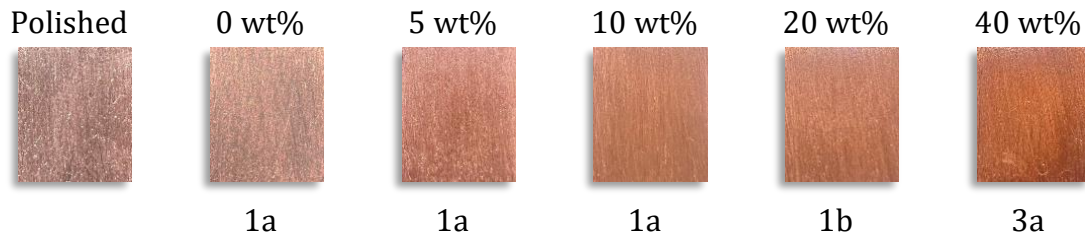


Figure 4: Corrosion of copper strips after immersion in SAE 5W-40 oil emulsions with different water concentrations.

Figure 5 illustrates the effect of emulsified water concentration on the friction and wear performance of SAE 5W-40 oil. Coefficient of friction (CoF) values in Figure 5(a) were derived from the slope of the friction force across the applied load range, with R^2 values exceeding 0.99. Reported data represent averaged results with a root mean squared error (RMSE) below 5%, ensuring high accuracy and repeatability.

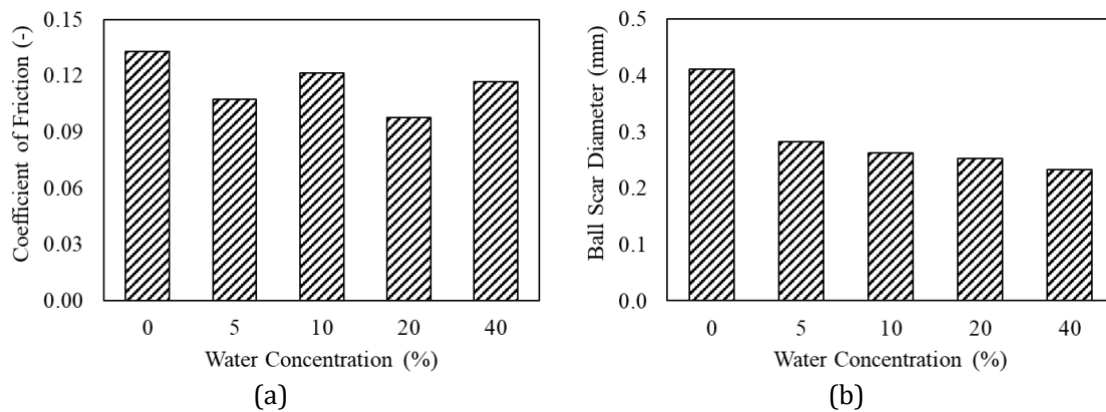


Figure 5: Effect of emulsified water concentration on (a) coefficient of friction and (b) ball scar diameter for SAE 5W-40 engine oil. Results indicate changes in friction and wear performance under simulated moisture contamination conditions.

Overall, adding water emulsions improves the frictional performance of the lubricant. The initial decrease in CoF at 5 wt% water indicates enhanced boundary lubrication, likely due to increased viscosity reducing asperity contact and friction. At 10 wt% water ingress, a slight increase in CoF is observed, potentially caused by emulsion destabilisation. The lowest CoF (~0.10), measured at 20 wt% water, represents a 26.6% reduction compared to neat SAE 5W-40, suggesting that a stable water-in-oil structure supports more effective boundary film formation. Beyond 20 wt%, further improvements plateau as water content approaches the lubricant's stability limit. The wear behaviour, indicated by the ball scar diameter in Figure 5(b), decreases steadily with increasing water content. This trend reflects the progressive enhancement of anti-

wear performance at higher water concentrations, attributed to the emulsion's increased viscosity and improved load-carrying capacity.

The lubrication behaviour observed in this study is consistent with established tribological mechanisms. At moderate water contamination levels (≤ 20 wt%), the increase in viscosity facilitated the formation of a more stable lubricant film, reducing asperity contact and thereby lowering both the coefficient of friction (CoF) and wear scar diameter (WSD). This trend reflects a transition from boundary to mixed lubrication, as reported in previous studies (Bosch & DellaCorte, 2024; Røn & Lee, 2014). However, beyond 20 wt% water, the mechanical advantages diminished as chemical degradation became dominant. The increased corrosivity could counteract the benefits of higher viscosity, leading to surface deterioration. This dual behaviour highlights a critical trade-off: while moderate emulsification may temporarily enhance load-carrying capacity, excessive water content could undermine long-term corrosion resistance and overall lubrication performance.

6.0 ELUCIDATION OF PHYSICOCHEMICAL AND FRICTION PROPERTIES

Adding water to SAE 5W-40 engine oil significantly influences its rheological and tribological behaviour. Up to 40 wt% water content, viscosity increases due to hydrogen bonding and microstructural rearrangements within the emulsion (Cafolla & Voïtchovsky, 2020). This behaviour is well captured by the VFT equation, which accurately describes the non-linear temperature–viscosity relationship across all samples. Among the fitted VFT parameters, the flow activation constant (B) reaches its maximum at 5 wt% water, indicating a temporary increase in flow resistance likely due to initial microstructural structuring. However, as water content increases, B declines, suggesting a shift toward more stabilised, less thermally sensitive emulsion behaviour.

This stabilising effect is further supported by the analysis of dimensionless viscosity gradients ($d\bar{\eta}/dT$), as shown in Figure 6. These gradients, calculated by normalising viscosity against the η_0 term from the VFT model, reflect the sensitivity of viscosity to temperature. All samples exhibit negative gradients, consistent with expected lubricant behaviour; however, the magnitude of the gradient decreases with both increasing temperature and water content. At 40 wt% water, the gradient approaches zero at higher temperatures (333–353 K), indicating a thermally resilient emulsion structure. In contrast, the sharp drop observed at 5 wt% water (-63 at 298 K) may represent a transitional instability, where the emulsion is highly sensitive to thermal perturbation.

Although the viscosity index (VI) could not be directly calculated due to the absence of kinematic viscosity and density data, the observed $d\bar{\eta}/dT$ trends provide a meaningful analogue. The reduced temperature sensitivity of viscosity at higher water concentrations, especially more than 20 wt%, is consistent with behaviour typically associated with high-VI lubricants (Bosch & DellaCorte, 2024). This suggests that water, beyond a certain threshold, increases viscosity and enhances its thermal stability, an advantageous trait for engine lubrication under variable temperature conditions.

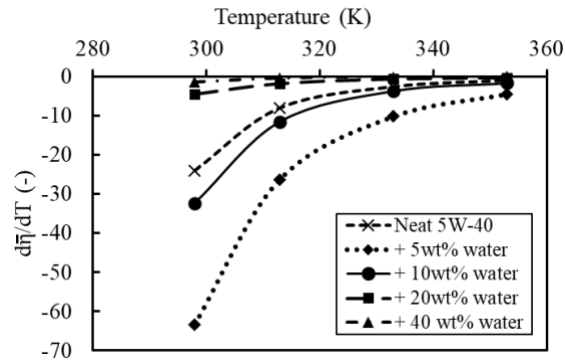


Figure 6: Non-dimensional derivative of viscosity ($d\eta/dT$) as a function of temperature for SAE 5W-40 oil blended with varying concentrations of deionised water.

From a tribological perspective, this viscosity enhancement translates to improved film thickness, reducing metal-to-metal contact under hydrodynamic lubrication. This helps suppress wear by providing a cushioning effect at the tribological interface, as observed with reduced wear scar diameters. However, the benefits of reduced friction and wear must be weighed against the increased corrosiveness observed at higher water contents. Water accelerates oxidative and acidic degradation of additives and metal surfaces, introducing chemical wear mechanisms that may dominate over time.

Therefore, while emulsified water can improve anti-wear performance through rheological stabilisation, it raises the risk of long-term chemical degradation. In the context of hydrogen-fuelled internal combustion engines (H_2 ICEs), where water vapour generation is inherent, this finding highlights the importance of lubricant formulation that balances viscosity, film strength, friction reduction, and corrosion resistance. Careful monitoring and additive design will be essential to manage this trade-off and ensure lubricant reliability in H_2 ICE applications.

While the results clearly show trends in friction, wear, and corrosion behaviour at different emulsification levels, it is recognised that the lack of surface characterisation tools, such as SEM/EDX and XPS, limits direct understanding of the mechanisms involved. These techniques could offer insights into tribofilm formation, material transfer, and chemical degradation at the interface. However, the current study focused on evaluating bulk properties to identify key performance thresholds. Future work will include these advanced surface analyses to understand the underlying tribological mechanisms better.

7.0 IMPACT OF VISCOSITY INCREASE ON ENERGY LOSSES AND ENVIRONMENTAL BURDEN

According to Chong et al. (2018), total frictional losses in a typical passenger car account for approximately 35.7% of the fuel energy input. Of this, 40% is attributed to in-cylinder friction, with 40% arising from hydrodynamic lubrication mechanisms such as piston skirt and journal bearing motion. Taking a proportional relationship, each 1% increase in lubricant viscosity could lead to a 1% increase in hydrodynamic friction. This characteristic equates to a 0.064% increase in total frictional losses for every 1% rise in viscosity.

Viscosity measurements in this study were taken at 100 °C, a representative bulk oil temperature for warmed-up internal combustion engines, including H₂ICEs. While localised hotspots may reach higher temperatures, 100 °C is an industry-standard reference for evaluating oil performance under typical operating conditions. Thus, as shown in Figure 2, dynamic viscosity of the emulsified lubricant at 100 °C increased by 28% to 257% for water concentrations ranging from 5 wt% to 40 wt%. This corresponds to an estimated 1.8% to 16.5% increase in frictional losses, which translates to an approximate 1–6% increase in total fuel consumption, assuming other factors remain constant.

Although seemingly modest, this increase becomes substantial when extrapolated to real-world use. In the case of conventional gasoline engines, for a typical passenger car consuming 7 L/100 km and driven 20,000 km annually:

1. A 1–6% increase in fuel use would result in 20–120 extra litres of fuel consumed per year per vehicle
2. This corresponds to 46–277 kg of additional CO₂ emissions annually, based on 2.31 kg CO₂ per litre of petrol burned
3. At current fuel prices (RM 2.00/L or USD \$1.20/L), this represents an added fuel cost of RM 40–240 (USD \$9–60) per year

At the fleet level, for every 1,000 vehicles, the cumulative impact could reach 120,000 additional litres of fuel consumed and over 277 tonnes of CO₂ emitted annually, illustrating the broader environmental and economic burden of uncontrolled water contamination in lubricants.

For H₂ICEs, although hydrogen combustion produces no tailpipe CO₂ emissions, increased viscosity still leads to higher hydrogen fuel consumption to overcome frictional losses. The environmental and economic burden then depends on the hydrogen production pathway:

1. Suppose the hydrogen is derived from renewable energy sources (green hydrogen). In that case, the impact is minimal in terms of greenhouse gas emissions, but the energy demand and hydrogen fuel cost would still increase.
2. For grey hydrogen (obtained from natural gas through steam methane reforming), increased hydrogen use indirectly leads to higher upstream CO₂ emissions, making friction-induced losses a significant environmental concern.
3. Additionally, since hydrogen costs more per unit of energy than gasoline, any efficiency loss results in higher fuel cost penalties, even without tailpipe carbon emissions.

CONCLUSIONS

This study simulated emulsified water conditions in SAE 5W-40 engine oil to reflect lubrication environments relevant to hydrogen-powered internal combustion engines (H₂ICEs). The results highlight that water incorporation or ingress significantly alters lubricant behaviour, with clear performance thresholds.

- (a) Viscosity increased with water content due to hydrogen bonding, with higher concentrations exhibiting VI-like thermal stability, as evidenced by diminished viscosity-temperature gradients.
- (b) The flow activation constant (*B*) from VFT equation peaked at 5 wt%, indicating transient thermal stabilisation, but declined at higher water levels, suggesting structural reorganisation within the emulsion.

- (c) Friction performance improved at moderate water content (≤ 20 wt%) due to more stable boundary lubrication, while further addition caused diminishing returns linked to emulsion instability.
- (d) Wear reduction was observed across all water levels, likely due to enhanced film thickness and load-carrying capacity.
- (e) Corrosion risk increased sharply beyond 20 wt%, signalling that chemical degradation may outweigh tribological gains at excessive water concentrations.

These findings highlight the importance of monitoring and controlling water content in engine oils, particularly for hydrogen-fuelled internal combustion engines (H₂ICEs), where water vapour is an inevitable combustion by-product. While emulsified water may offer short-term tribological benefits, such as improved viscosity and cushioning effect, it can also significantly increase frictional losses and chemical degradation over time. Thus, a careful balance between tribological performance and chemical stability must be maintained through informed lubricant formulation, additive design, and operational monitoring strategies.

REFERENCES

- Amat Ventayol, A., Lam, J. S. L., Bai, X., & Chen, Z. S. (2025). Comparative life cycle assessment of hydrogen internal combustion engine and fuel cells in shipping. *International Journal of Hydrogen Energy*, 109, 774–788. <https://doi.org/10.1016/j.ijhydene.2025.02.150>
- Ayeni, A. O., Tagwai, S., Dick, D. T., Agboola, O., Ayoola, A. A., Babatunde, D. E., & Oni, B. A. (2021). A two-stage coupling process for the recovery of base oils from used lubricating oils. *IOP Conference Series: Earth and Environmental Science*, 655(1). <https://doi.org/10.1088/1755-1315/655/1/012029>
- Bhosale, A. A., Joshi, K., Karadkar, T., Mangidkar, K., & Mundhe, P. (2014). Analysis of lubricating oil deterioration in four-wheeler. *Applied Mechanics and Materials*, 446–447, 558–561. <https://doi.org/10.4028/www.scientific.net/AMM.446-447.558>
- Bosch, J., & DellaCorte, C. (2024). Rheological Characterization and Tribological Evaluation of Water-Based Lubricants in AISI 52100 Bearing Steel. *Tribology Letters*, 72(1). <https://doi.org/10.1007/s11249-023-01811-7>
- Butcher, R., Bradley, N., & Powell, T. (2023). Real Time Observations of Water Entering and Leaving Internal Combustion Engine Oil, Over Both Standard Engine, ICE and Plug-in Hybrid, PHEV Dynamic Drive-Cycles. *SAE Technical Paper*.
- Cafolla, C., & Voitchovsky, K. (2020). Impact of water on the lubricating properties of hexadecane at the nanoscale. *Nanoscale*, 12(27), 14504–14513. <https://doi.org/10.1039/d0nr03642k>
- Chen, K., Seo, D., & Canteenwalla, P. (2021). The effect of high-temperature water vapour on degradation and failure of hot section components of gas turbine engines. In *Coatings* (Vol. 11, Issue 9). MDPI. <https://doi.org/10.3390/coatings11091061>
- Chong, W. W. F., Ng, J. H., Rajoo, S., & Chong, C. T. (2018). Passenger transportation sector gasoline consumption due to friction in Southeast Asian countries. *Energy Conversion and Management*, 158, 346–358. <https://doi.org/10.1016/j.enconman.2017.12.083>
- Garca-Coln, L. S., del Castillo, L. F., & Goldstein, P. (1989). Theoretical basis for the Vogel-Fulcher-Tammann equation. *PHYSICAL REVIEW B*, 40. <https://doi.org/10.1103/PhysRevB.40.7040>

- Hemmat Esfe, M., Motallebi, S. M., & Toghraie, D. (2022). Optimal viscosity modelling of 10W40 oil-based MWCNT (40%)-TiO₂ (60%) nanofluid using Response Surface Methodology (RSM). *Heliyon*, 8(12). <https://doi.org/10.1016/j.heliyon.2022.e11944>
- Lee, C. T., Lee, M. B., Chong, W. W. F., Ng, J. H., Wong, K. J., & Chong, C. T. (2022). Boundary Lubricity of Vegetable-Oil-Derived Trimethylolpropane (TMP) Ester. *Lubricants*, 10(12). <https://doi.org/10.3390/lubricants10120346>
- Mohamed Ariffin, N. A. A., & Chong, W. W. F. (2024). ASSESSING THE TRIBOLOGICAL PERFORMANCE OF POLYALPHAOLEFIN UNDER ELECTRICAL CURRENT CONDITIONS. *Journal of Transport System Engineering*, 11(1), 35–40. www.jtse.utm.my
- Mohamed Ariffin, N. A. A., Lee, C. T., Thirugnanasambandam, A., Wong, K. J., & Chong, W. W. F. (2024). Triboelectric Performance of Ionic Liquid, Synthetic, and Vegetable Oil-Based Polytetrafluoroethylene (PTFE) Greases. *Lubricants*, 12(8). <https://doi.org/10.3390/lubricants12080272>
- Musa Abubakar, A., Hamisu, A., & Aminu, K. S. (2018). Viscometric Study of PEG-400 in Aqueous and Non Aqueous. *International Journal of Science and Research*. <https://doi.org/10.21275/ART20202661>
- Noori, S., Diamanti, M. V., Pedferri, M. P., Brenna, A., Ormellese, M., Noori, S., Diamanti, M. V., Pedferri, M., Brenna, A., & Ormellese, M. (2018). Effect of water content on the corrosiveness of imidazolium-based ionic liquids.
- Onorati, A., Payri, R., Vaglieco, B. M., Agarwal, A. K., Bae, C., Bruneaux, G., Canakci, M., Gavaises, M., Günthner, M., Hasse, C., Kokjohn, S., Kong, S. C., Moriyoshi, Y., Novella, R., Pesyridis, A., Reitz, R., Ryan, T., Wagner, R., & Zhao, H. (2022). The role of hydrogen for future internal combustion engines. In *International Journal of Engine Research* (Vol. 23, Issue 4, pp. 529–540). SAGE Publications Ltd. <https://doi.org/10.1177/14680874221081947>
- Rahmani, R., Dolatabadi, N., & Rahnejat, H. (2023). Multiphysics performance assessment of hydrogen fuelled engines. *International Journal of Engine Research*, 24(9), 4169–4189. <https://doi.org/10.1177/14680874231182211>
- Røn, T., & Lee, S. (2014). Influence of temperature on the frictional properties of water-lubricated surfaces. *Lubricants*, 2(4), 177–192. <https://doi.org/10.3390/lubricants2040177>
- Sazzad, M. R. I., Rahman, M. M., Hassan, T., Al Rifat, A., Al Mamun, A., Adib, A. R., Meraz, R. M., & Ahmed, M. (2024). Advancing sustainable lubricating oil management: Re-refining techniques, market insights, innovative enhancements, and conversion to fuel. In *Heliyon* (Vol. 10, Issue 20). Elsevier Ltd. <https://doi.org/10.1016/j.heliyon.2024.e39248>
- Sharma, A., Gupta, G., & Agrawal, A. (2020). Utilization of Waste Lubricating Oil as a Diesel Engine Fuel. *IOP Conference Series: Materials Science and Engineering*, 840(1). <https://doi.org/10.1088/1757-899X/840/1/012015>
- Shi, Y., & Larsson, R. (2016). Non-corrosive and Biomaterials Protic Ionic Liquids with High Lubricating Performance. *Tribology Letters*, 63(1). <https://doi.org/10.1007/s11249-016-0692-9>
- Stępień, Z. (2021). A comprehensive overview of hydrogen-fueled internal combustion engines: Achievements and future challenges. In *Energies* (Vol. 14, Issue 20). MDPI. <https://doi.org/10.3390/en14206504>
- Vasishth, A., Kuchhal, P., & Anand, G. (2014). Study of Rheological Properties of Industrial Lubricants. *Conference Papers in Science*, 2014, 1–5. <https://doi.org/10.1155/2014/324615>

- Wang, L., Li, X., Hong, C., Guo, P., Guo, S., & Yang, Z. (2023). Research and Development of Hydrogen-Fueled Internal Combustion Engines in China. In ACS Omega (Vol. 8, Issue 51, pp. 48590–48612). American Chemical Society. <https://doi.org/10.1021/acsomega.3c05397>
- Zhou, Z., Zhou, X., Huang, Q., Liu, X., Wang, L., & Xing, S. (2024). Impact of oil-water emulsions on lubrication performance of ship stern bearings. Scientific Reports, 14(1). <https://doi.org/10.1038/s41598-024-83253-2>